Quadratic Nonlinear Optical Response in Partially Charged Donor-Substituted Tetrathiafulvalene: From a Computational Investigation to a Rational Synthetic Feasibility

Jean François Lamère, Isabelle Malfant, Alix Sournia-Saquet, and Pascal G. Lacroix*

Laboratoire de Chimie de Coordination du CNRS, 205 route de Narbonne, 31077 Toulouse, France

Jean Marc Fabre, Lakhémici Kaboub, and Tahar Abbaz

Laboratoire de Chimie Organique: Hétérochimie et Matériaux Organiques, UMR 5076, ENSCM 8 rue de l'Ecole Normale, 34296 Montpellier cedex 5, France

Abdel-Krim Gouasmia

Laboratoire de Chimie des Matériaux Organiques, Centre universitaire de Tebessa, Route de Constantine, 12000 Tebessa, Algerie

Inge Asselberghs and Koen Clays

Department of Chemistry, University of Leuven, Celestjnenlaan 200D, 3001 Leuven, Belgium

Received September 27, 2006. Revised Manuscript Received November 16, 2006

A computational (ZINDO) investigation is employed to estimate the molecular hyperpolarizability (β) of a [(TTF−NH_2)$_8$] (TTF = tetrathiafulvalene) octameric stack at various fractional ($0 < \rho < 1$) oxidation states of $TTF^{\rho+}$. While the neutral [(TTF−NH_2)$_8$] octamer exhibits a modest (7.6×10^{-30} cm^5 esu^{-1}) static β_0 value, in relation to a nearly centrosymmetric electronic structure, the formal $(TTF-NH_2)^{0.25+}$ oxidation state leads to a giant ($\beta_0 = 3891 \times 10^{-30}$ cm^5 esu^{-1} per octamer) NLO response. This effect is related to the appearance of an extremely intense HOMO → LUMO-based low-lying transition, occurring at 1260 nm upon fractional oxidation, thus providing new and unexpected interest in TTF-donor substituted molecules. To illustrate the chemical feasibility of such species, two kinds of derivatives are synthesized: a TTF-dimethylaniline **(TTF-DMA)** by using in particular a Suzuki cross-coupling reaction between iodo-TTF and *p*-dimethylaminophenylboronic acid and a TTF-vinyldimethylaniline **(TTF-VDMA)** by a Wittig-type condensation notably between TTF-carboxaldehyde and *p*-(dimethylamino)benzyltriphenylphosphonium bromide. Their NLO response, evaluated at 1.064 μm by the Hyper Raleigh Scattering technique, leads to β values around 240×10^{-30} cm^5 esu^{-1}, in both cases. Additionally, these monomeric species are observed to exhibit very strong multiphoton fluorescence in solution after one electron oxidation. Different routes are discussed toward a possible engineering of TTF-donor based chromophores into oligomeric stacks in the solid state.

Introduction

The last few decades have witnessed a growing interest for molecular materials and have led to the design of intriguing new magnets,[1] conductors and superconductors,[2] photochromic crystals,[3] or nonlinear optical (NLO) materials.[4,5] One reason for this interest is the expectation that, in molecular materials, several electronic behaviors could be combined in a single molecular entity, thus providing a route toward advanced functionalized materials with switchable properties or hybrid magnetic-conducting-optical electronic capabilities.[6]

In the search toward multiproperty molecular materials, the question of what properties to combine and how is the first one to address. For instance, providing a simple rationale for linking nonlinear optics and magnetism is hampered by the fact that NLO materials are traditionally regarded within the framework of dielectrics subjected to intense electric fields (dipole approximation). Therefore, the molecular hyperpolarizability (β) is assumed not to depend on any magnetic stimulus.[7] Indeed, only few reports have focused on nonlinear optics in paramagnetic species,[8,9] or in magnetized media.[10] By contrast, NLO properties and electron

(1) Kahn, O. *Molecular Magnetism*; VCH: Weinheim, 1993. Miller, J. S.; Epstein, A. J. *Angew. Chem., Int. Ed. Engl.* **1994**, *33*, 385.
(2) See for example: Special Issue on Molecular Conductors. *J. Mater. Chem.* **1995**, *5* (10).
(3) Photochromism: Memories and Switches, a special issue of *Chem. Rev.* **2000**, *100* (May).
(4) Optical Nonlinearity in Chemistry, a special issue of *Chem. Rev.* **1994**, *94* (Jan).
(5) (a) *Molecular Nonlinear Optics: Materials, Physics and Devices;* Zyss, J., Ed.; Academic Press: Boston, 1994. (b) *Nonlinear Optics of Organic Molecules and Polymers*; Nalwa, H. S., Miyata, S., Eds; CRC Press: New York, 1997.
(6) (a) Lacroix, P. G. *Chem. Mater.* **2001**, *13*, 3495. (b) Bousseksou, A.; Molnár, G.; Matouzenko, G. *Eur. J. Inorg. Chem.* **2004**, 4353.
(7) Prasad, P. N.; Williams, D. J. *Introduction to Nonlinear Optical Effects in Molecules and Polymers*; J. Wiley: New York, 1991; pp 8−34.

10.1021/cm0623110 CCC: $37.00
Published on Web 01/23/2007

Scheme 1

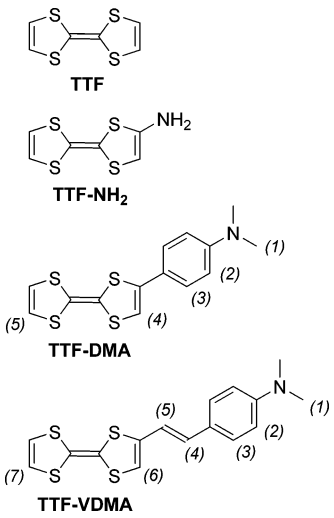

conduction seem to be naturally related, as both behaviors are based on the same general concept of charge transfer: an intermolecular charge transfer along stacks of ions in the case of conducting materials,[11] and an intramolecular ("push−pull") charge transfer between a donor and an acceptor counterpart in NLO chromophores.[12] The possibility of π-overlaps between the ions could modulate the overall electronic structure, thus providing the link between the properties. Therefore, one may expect that the same "building blocks" could be used for both purposes, depending on their capability to be engineered in a suitable solid-state environment.

For example, tetrathiafulvalene (TTF, Scheme 1) has been the basis of various highly conducting charge-transfer complexes, including the first organic conductor in 1973.[13,14] In these systems, TTF acts as an electron donor, in relation to its capability to be reversibly oxidized into a radical cation.[11,15,16] The possibility of using TTF derivatives in nonlinear optics has first been reported in 1997 by Andreu et al.[17] and has then been reviewed.[18] By contrast versus traditional NLO chromophores, TTF-based materials possess several additional properties, which have deserved very limited attention, in a perspective of nonlinear optics: (*i*) first, the crystal structures reveal a trend for highly overlapping TTF species with potential "through space" charge transfers, a possibility which has previously been envisioned for providing new NLO capabilities.[19−21] (*ii*) Then, TTF units are frequently observed to carry formal ($0 < \rho < 1$) fractional charge, in the solid state. From a theoretical point of view, this should allow access to a relationship between β and ρ, an intriguing issue which, up to now, has never been addressed. Furthermore, fractional charge transfers usually imply enhanced charge delocalizations, and one may expect this situation to lead to NLO responses of greater magnitude than those of the traditional ($\rho = 0$, and 1) situations. These considerations illustrate the fact that TTF-based chromophores could provide NLO materials of much greater electronic capabilities than those of the standard donor−acceptor substituted stilbenes widely investigated during the 1980s and 1990s.[4,5]

Following this initial idea, we have been interested in a computational investigation of the benchmark TTF−NH_2 derivative (Scheme 1). It must be emphasized that this molecule has never been reported either experimentally or theoretically. At this stage, it was selected on the basis of two simple criteria: (*i*) the formal introduction of two atoms (N and H) provides a modest modification of the TTF shape, which leads to the crude but reasonable starting assumption that the intermolecular interactions in TTF−NH_2 stacks should be reminiscent of those observed in TTF-based crystal structures, where the S···S contacts are dominant. (*ii*) NH_2 as well as TTF exhibits donor capabilities. Therefore, TTF−NH_2 should not be subjected to sizable charge-transfer processes upon electron excitation and should possess very modest NLO capabilities in its neutral form, thus allowing β to be directly related to ρ, after partial oxidation.

The organization of this article is the following: A semiempirical computation of the NLO response of a stack built up from 8 TTF−NH_2 units will first be presented and discussed as a function of the fractional charge to point out that the β optimization is achieved at low oxidation states of the TTF units. Then, the target donor-substituted TTF-dimethylaminoaniline and TTF-vinyldimethylaniline (**TTF-DMA** and **TTF-VDMA** in Scheme 1) will be presented to illustrate the synthetic feasibility of such donor-substituted species, and their NLO properties will be examined. Finally, the possibilities for designing oligomeric TTF stacks stabilized in the partial oxidation state will be discussed in a perspective of hybrid material combining electron delocalization and NLO response.

Experimental Section

Starting Materials and Equipment. Tributylstannyltetrathiafulvalene **1a**,[22a] and its methylated derivatives **1b** and **1c**,[22b,c]

(8) Di Bella, S.; Fragalà, I.; Ledoux, I.; Marks, T. J. *J. Am. Chem. Soc.* **1995**, *117*, 9481.
(9) (a) Averseng, F.; Lacroix, P. G.; Malfant, I.; Périssé, N.; Lepetit, C.; Nakatani, K. *Inorg. Chem.* **2001**, *40*, 3797. (b) Margeat, O.; Lacroix, P. G.; Costes, J. P.; Donnadieu, B.; Lepetit, C.; Nakatani, K. *Inorg. Chem.* **2004**, *43*, 4743.
(10) (a) Lacroix, P. G.; Clément, R.; Nakatani, K.; Zyss, J.; Ledoux, I. *Science* **1994**, *263*, 658. (b) Benard, S.; Yu, P.; Audiere, J. P.; Riviere, E.; Clement, R.; Guilhem, J.; Tchertanov, L.; Nakatani, K. *J. Am. Chem. Soc.* **2000**, *122*, 9444.
(11) Wudl, F. *Acc. Chem. Res.* **1984**, *17*, 227.
(12) Williams, D. J. *Angew. Chem., Int. Ed. Engl.* **1984**, *23*, 690.
(13) Ferraris, J. P.; Cowan, D. O.; Valatka, V.; Perlstein, J. H. *J. Am. Chem. Soc.* **1973**, *95*, 948.
(14) For a review on highly conducting materials based on TTF, see: Fabre, J. M. *J. Solid. State Chem.* **2002**, *168*, 367 and references therein.
(15) Kodorkovsky, V.; Becher, J. Y. *Organic Conductors*; Farges, J. P., Ed.; Marcel Dekker: New York, 1994.
(16) Carcel, C.; Fabre, J. M. *Synth. Met.* **2002**, *130*, 99.
(17) Andreu, R.; de Lucas, A. I.; Garín, J.; Martín, N.; Orduna, J.; Sanchez, L.; Seoane, C. *Synth. Met.* **1997**, *86*, 1817.
(18) Segura, J. L.; Martín, N. *Angew. Chem., Int. Ed.* **2001**, *40*, 1372.
(19) For an early computational investigation of "through space charge transfer", see: Di Bella, S.; Fragalà, I.; Ratner, M. R.; Marks, T. J. *J. Am. Chem. Soc.* **1993**, *115*, 682.
(20) Zyss, J.; Ledoux, I.; Volkov, S.; Cheryak, V.; Mukamel, S.; Bartholomew, G. P.; Bazan, C. *J. Am. Chem. Soc.* **2000**, *122*, 11956.
(21) Lacroix, P. G.; Padilla-Martínez, I. I.; López Sandoval, H.; Nakatani, K. *New J. Chem.* **2004**, *28*, 542.
(22) (a) Iyoda, M.; Kuwatani, Y.; Ueno, N.; Oda, M. *J. Chem. Soc., Chem. Commun.* **1992**, 158. (b) Bouguessa, S.; Gouasmia, A. K.; Golhen, S.; Ouahab, L.; Fabre, J. M. *Tetrahedron Lett.* **2003**, *44*, 9275. (c) Iyoda, M.; Fukuda, M.; Sasaki, S.; Yoshida, M. *Synth. Met.* **1995**, *70*, 1171.

iodotetrathiafulvalene **1′**,[23] tetrathiafulvalene-carboxaldehyde **5a**,[24] and *p*-(dimethylamino)benzyltriphenylphosphonium bromide[25] were prepared as described in the literature. ^{1}H NMR spectra were recorded on a Brucker AC 250 spectrophotometer. The atom labeling used for the assignment of **TTF-DMA** and **TTF-VDMA** is given in Scheme 1. The chemical shifts δ are in ppm and the coupling constant J in Hz. UV−visible spectra were recorded with a Hewlett-Packard 8452A spectrophotometer. Elemental analyses were performed by the "Service de Microanalyses du Laboratoire de Chimie de Coordination" (Toulouse) with a Perkin-Elmer 2400 Serie II instrument.

Theoretical Methods. The all-valence INDO (intermediate neglect of differential overlap) method,[26,27] in connection with the sum over state (SOS) formalism,[28] was employed for the calculation of the electronic spectra and β_0, static molecular hyperpolarizabilities of $[(TTF-NH_2)_8]^{q+}$, for $q = 0$, 2, 4, 6, and 8. The restricted Hartree−Fock (RHF) procedure was employed in all cases. Details for the computationally efficient INDO−SOS-based method for describing molecular optical nonlinearities have been reported elsewhere.[29] In the present approach, the monoexcited configuration interaction (MECI) approximation was employed to describe the excited states. The highest 30 occupied orbitals and the lowest 30 unoccupied ones were selected to undergo CI mixing, and the lowest 400 resulting energy transitions were used for the SOS procedure. We have checked that using 400 transitions is sufficient to reach β convergence. All calculations were performed using the INDO/1 Hamiltonian incorporated in the commercially available software package ZINDO.[30] The geometry used for the calculations of the $[TTF-NH_2]_8$ octamer was built up from the previously reported X-ray structures of TTF-TCNQ.[31] Additional calculations were performed for various stacking distances (cell parameter $b = 3.819$ Å in the TTF-TCNQ crystal structure) ranging from $b = 3.619$ to $b = 4.019$ Å, to verify that the results are not qualitatively affected by changing the stacking distance. No further optimization of the intermolecular interactions was performed. The $[TTF-NH_2]_8$ octamer used in the computational approach is shown in Figure 1. Computed hyperpolarizabilities are static β_0 calculated at zero frequency ($E = 0$, $\lambda = \infty$), in any case. However, they will be simply labeled β, for simplification.

Syntheses. ***4a*** *(TTF-DMA) (Scheme 2). (1) Route a.* To a stirred solution of tributylstannyltetrathiafulvalene **1a** (390 mg, 0,79 mmole, 1.0 equiv) in dry toluene under nitrogen were added 1.1 equiv of 1-bromo-4-(dimethylamino)benzene and tetrakis-triphenylphosphine palladium $[Pd(PPh_3)_4]$ (10 mol %). The reaction mixture was refluxed for 72 h under nitrogen and then concentrated in vacuo. The residue was purified by chromatography on silica gel eluting with hexane-dichloromethane (2:1) to provide (12%) the expected **TTF-DMA 4a** as a dark yellow crystalline solid. ^{1}H NMR ($CDCl_3$): δ 2.96 (6H, s, H_1); 6.24 (1H, s, H_4); 6.31 (2H, s, H_5, H_6); 6.65 (2H, d, $J = 8.6$ Hz, H_3); 7.27 (2H, d, $J = 8.8$ Hz, H_2). MS (FAB^+): 323 (M^+). Anal. Calcd for $C_{14}H_{13}NS_4$ (323.49): C, 51.98; H, 4.05; N, 4.33. Found: C, 52.13; H, 3.59; N, 4.24. Single crystals suitable for X-ray diffraction studies were obtained by slow evaporation in acetonitrile.

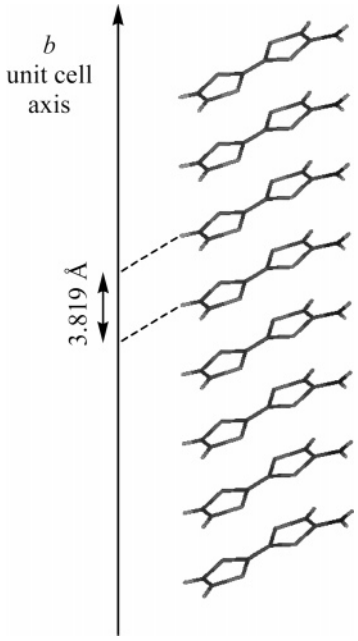

Figure 1. $[(TTF-NH_2)_8]$ octameric entity used for the β_0 calculation.

(2) Route b. To a mixture of iodotetrathiafulvalene (**1′**) (286 mg, 0.866 mmol, 1.0 equiv) and $[Pd(PPh_3)_4]$ (10 mol %) in 10 mL of dry toluene under nitrogen was added 4-(dimethylamino)phenylboronic acid (160 mg, 0.96 mmole, 1.1 equiv), followed by a solution of sodium carbonate (183 mg, 1.732 mmole, 2 equiv) in 2 mL of water. After a 72 h reflux at 110 °C, the reaction mixture was cooled down, diluted with CH_2Cl_2, and washed with brine. The organic phase was separated and dried over $MgSO_4$. The solvent was removed under reduced pressure and the residue was purified by chromatography, with hexane-CH_2Cl_2 (2:1), affording the desired **TTF-DMA** as a dark yellow crystalline solid (yield: 22%).

4b *and* ***4c*** *(Scheme 2). (1) Route c: General Procedure for Compounds* ***2b*** *and* ***2c****.* To a stirred solution of tributylstannyltetrathiafulvalene **1** (1.0 equiv) in dry toluene under nitrogen were added dropwise 1.1 equiv of 1-bromo-4-nitrobenzene and then tetrakis-triphenylphosphine palladium $[Pd(PPh_3)_4]$ (0.05 equiv). The reaction mixture was refluxed for 60 h under nitrogren and then concentrated in vacuo. The residue was chromatographed on a silica column with hexane-dichloromethane (3:1) to afford the expected compound **2** as a solid.

2b: Dark violet powder (98%), mp 168 °C. ^{1}H NMR ($CDCl_3$): δ 1.96 (6H, s, $2CH_3$); 2.08 (3H, s, CH_3); 7.52 ($2H_{arom.}$, d, $J = 8.82$ Hz); 8.23 ($2H_{arom.}$, d, $J = 8.82$ Hz). MS (FAB^+): 367 (M^+). Anal. Calcd for $C_{15}H_{13}NO_2S_4$: C, 49.04; H, 3.54; N, 3.81. Found: C, 50.16; H, 3.01; N, 3.12.

2c: Dark violet powder (96%), mp 156 °C. ^{1}H NMR ($CDCl_3$): δ 2.08 (3H, s, CH_3); 2.17 (3H, s, CH_3); 5.89 (1H, s, C=CH); 7.52 ($2H_{arom.}$, d, $J = 8.76$ Hz); 8.24 ($2H_{arom.}$, d, $J = 8.73$ Hz). MS (FAB^+): 353 (M^+). Anal. Calcd for $C_{14}H_{11}NO_2S_4$: C, 45.59; H, 3.11; N, 3.96. Found: C, 45.32; H, 3.05; N, 4.12.

(2) General Procedure for Compounds ***3b*** *and* ***3c****.* A stirred mixture of 4-nitrophenyltetrathiafulvalene **2** (1 equiv), tin (2 equiv), and aqueous solution of HCl (35%) (0.6 mL, 5 equiv) in ethanol (30 mL) was refluxed for 4 h under nitrogen. During this time the initial black solution turned light yellow. The solution was then concentrated in vacuo and treated with an aqueous solution (100

(23) Wang, C.; Ellern, A.; Khodorkovsky, V.; Bernstein, J.; Becker, J. Y. *J. Chem. Soc., Chem. Commun.* **1994**, 983.
(24) Garin, J.; Orduna, J.; Uriel, S.; Moore, A. J.; Bryce, M. R.; Wegener, S.; Yufit, D. S.; Howard, J. A. K. *Synthesis* **1994**, 489.
(25) Chou, S. S. P.; Yeh, Y. H. *Tetrahedron Lett.* **2001**, *42*, 1309.
(26) Pople, J. A.; Beveridge, D. L.; Dobosh, P. A. *J. Chem. Phys.* **1967**, *47*, 2026.
(27) (a) Zerner, M.; Loew, G.; Kirchner, R.; Mueller-Westerhoff, U. *J. Am. Chem. Soc.* **1980**, *102*, 589. (b) Anderson, W. P.; Edwards, D.; Zerner, M. C. *Inorg. Chem.* **1986**, *25*, 2728.
(28) Ward, J. F. *Rev. Mod. Phys.* **1965**, *37*, 1.
(29) Kanis, D. R.; Ratner, M. A.; Marks, T. J. *Chem. Rev.* **1994**, *94*, 195.
(30) *ZINDO*, release 96.0; Molecular Simulations Inc.: Cambridge, U.K., 1996.
(31) Kistenmacher, T. J.; Phillips, T. E.; Cowan, D. O. *Acta Crystallogr., Sect. B: Struct. Crystallogr. Cryst. Chem.* **1974**, *30*, 763.

Scheme 2

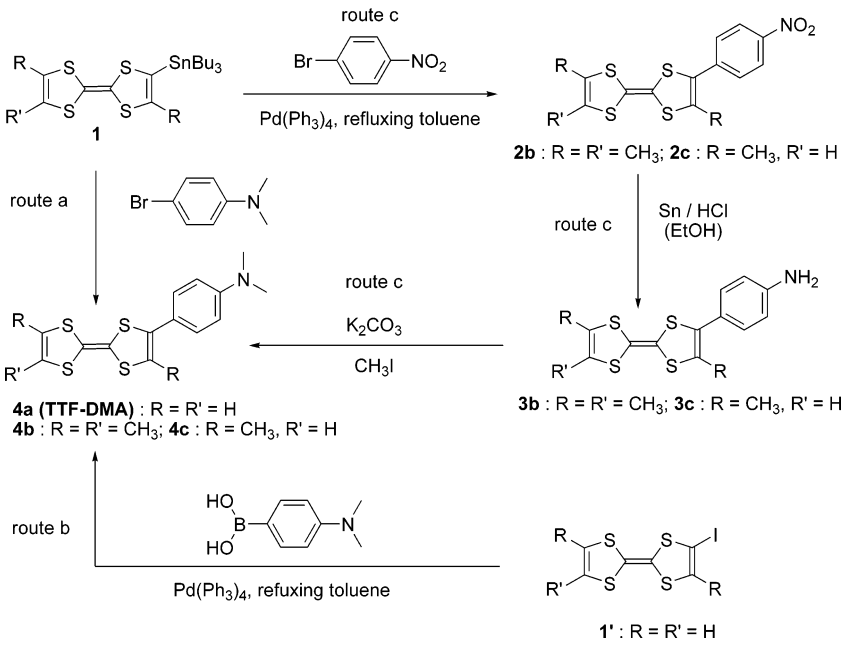

Scheme 3

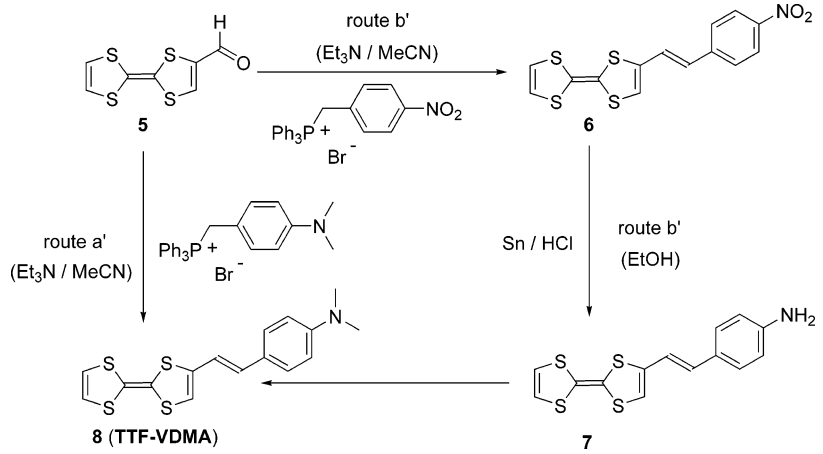

mL) of sodium hydroxide (0.1 M) and extracted with ether. The organic phase was washed with water, dried ($MgSO_4$), and concentrated in vacuo. The product was subjected to column chromatography on silica (CH_2Cl_2), affording the expected compound **3** as a powder.

3b: Brown powder (65%), mp 147 °C. ^{1}H NMR ($CDCl_3$): δ 1.93 (6H, s, $2CH_3$); 2.15 (3H, s, CH_3); 3.50−3.95 (2H, m, NH_2); 6.63 ($2H_{arom}$., d, J = 8.46 Hz); 7.11 ($2H_{arom}$., d, J = 8.44 Hz). MS (FAB$^+$): 337 (M^+). Anal. Calcd for $C_{15}H_{15}NS_4$: C, 53.41; H, 4.45; N, 4.15. Found: C, 53.30; H, 4.24; N, 3.95.

3c: Red brown powder (62%), mp 163 °C. ^{1}H NMR ($CDCl_3$): δ 1.95 (3H, s, CH_3); 2.02 (3H, s, CH_3); 3.48−3.85 (2H, m, NH_2); 5.80 (1H, s, C═CH); 6.60 ($2H_{arom}$., d, J = 8.49 Hz); 7.09 ($2H_{arom}$., d, J = 8.51 Hz). MS (FAB$^+$): 323 (M^+). Anal. Calcd for $C_{14}H_{13}NS_4$: C, 52.01; H, 4.02; N, 4.34. Found: C, 51.28; H, 3.91; N, 4.51.

*(3) General Procedure for Compounds **4b** and **4c***. To a stirred solution of 4-aminophenyltetrathiafulvalene **3** (1 equiv) and of iodomethane (4 equiv) in acetone (15 mL) under nitrogen was added K_2CO_3 (2 equiv). After 4 days of stirring at room temperature, the precipitate obtained was filtered, washed with acetone, and then extracted with CH_2Cl_2. The organic phase was dried ($MgSO_4$) and concentrated in vacuo, providing the expected compound **4** as a colored powder.

4b: Orange powder (78%), mp 202 °C. ^{1}H NMR ($CDCl_3$): δ 1.99 (6H, s, $2CH_3$); 2.09 (3H, s, CH_3); 3.37 (6H, s, NMe_2); 7.71 (2H, d, J = 8.88 Hz); 8.07 (2H, d, J = 8.86 Hz). MS (FAB$^+$): 365 (M^+). Anal. Calcd for $C_{17}H_{19}NS_4$: C, 55.89; H, 5.20; N, 3.83. Found: C, 55.12; H, 4.99; N, 3.95.

4c: Red brown powder (74%), mp 181 °C. H^1-NMR ($CDCl_3$): δ 2.09 (3H, s, CH_3); 2.11 (3H, s, CH_3); 3.37 (6H, s, NMe_2); 5.79 (1H, s, CH═C); 7.71 ($2H_{arom}$., d, J = 8.88 Hz); 8.07 ($2H_{arom}$., d, J = 8.96 Hz). MS (FAB$^+$): 351 (M^+). Anal. Calcd for $C_{16}H_{17}NS_4$: C, 54.70; H, 4.84; N, 3.99. Found: C, 54.21; H, 4.12; N, 4.08.

8 (TTF-VDMA): 2-(4-dimethylaminophenyl)-1-(tetrathiafulvalenyl)ethene) (Scheme 3). *(1) Route a′*. To a suspension of *p*-(dimethylamino)benzyltriphenylphosphonium bromide (1.84 g, 3.86 mmol, 3 equiv) and TTF-carboxaldehyde **5** (300 mg, 1.29 mmol, 1 equiv) in 30 mL of dry acetonitrile under nitrogen was added triethylamine (2.16 mL, 12 equiv). The reaction mixture was refluxed for 4 h under nitrogen and then concentrated in vacuo. The residue was purified by chromatography on silica eluting with hexane-CH_2Cl_2 (2:1) to afford the expected compound **TTF-VDMA 8** (44%), as a yellow crystalline solid. ^{1}H NMR ($CDCl_3$): δ 2.97 (6H, s, H_1); 6.20 (1H, s, H_6); 6.31 (2H, s, H_7, H_8); 6.34 (1H, d, J = 15.6 Hz, H_4); 6.66 (2H, d, J = 8.6 Hz, H_3); 6.68 (1H, d, J = 16.2 Hz, H_5); 7.28 (2H, d, J = 8.8 Hz, H_2). MS (FAB$^+$): 349 (M^+). Anal. Calcd for $C_{16}H_{15}NS_4$ (349.53): C, 54.98; H, 4.33; N,

Table 1. Crystal Data for TTF-DMA and TTF-VDMA

	TTF-DMA	TTF-VDMA
Crystal Data		
chemical formula	$C_{14}H_{13}NS_4$	$C_{16}H_{15}NS_4$
mol.wt.	323.49	349.53
crystal size (mm)	0.05 × 0.25 × 0.3	0.05 × 0.25 × 0.3
crystal system	monoclinic	monoclinic
space group	$P2_1$	$P2_1$
a (Å)	6.552(2)	6.7577(5)
b (Å)	8.074(2)	7.8823(9)
c (Å)	14.253(7)	15.7512(12)
β (deg)	91.23(5)	93.660(9)
V (Å^3)	753.9(5)	837.30(13)
Z	2	2
P_{calc} (Mg/m^3)	1.425	1.386
μ (Mo Kα) (mm^{-1})	0.615	0.559
Data Collection		
temperature (K)	293	293
radiation (Mo Kα) (Å)	0.71073	0.71073
scan mode	f	f
θ range (deg)	2.86 < θ < 26.09	2.59 < θ < 26.01
no. of reflections		
measured	7549	8424
unique	2946	3148
Refinement		
refinement on	F^2	F^2
no. of variables	172	218
H-atom treatment	calculated	mixed
R [$I > 2\sigma(I)$]	0.1126	0.0317
wR2	0.2619	0.0587
Flack parameter	1.1(6)	0.03(9)
$\Delta\rho_{max}$ (e Å^{-3})	+0.429	+0.171
$\Delta\rho_{min}$ (e Å^{-3})	−0.344	−0.209
GOF	0.773	0.917

4.01. Found: C, 55.00; H, 3.96; N, 4.97. Single crystals suitable for X-ray diffraction studies were obtained by slow evaporation in acetonitrile.

(2) Route b′. Compound **6** was obtained with a trans configuration as described in the literature,[32] exhibiting the same physical and spectroscopic characteristics.

Compound **7** was prepared by using the same experimental process as **3b** and **3c** from 1 equiv of 2-(4-nitrophenyl)-1-(tetrathiafulvalenyl)ethene **6.**

7: Light brown powder (65%). ^{1}H NMR ($CDCl_3$): δ 6.25 (2H, s, CH═CH); 6.30 (1H, s, CH═C); 6.52 (1H, d, J = 15.45 Hz); 6.63 (2H$_{arom}$., d, J = 8.40 Hz); 7.05 (1H, d, J = 15.65 Hz); 7.15 (2H$_{arom}$., d, J = 8.40 Hz). MS (FAB$^+$): 321 (M$^+$). Anal. Calcd for $C_{14}H_{11}NS_4$: C, 52.34; H, 3.42. Found: C, 52.15; H, 3.37.

Compound **8** was synthesized by employing the same experimental process as **4b** and **4c** from 1 equiv of 2-(4-aminophenyl)-1-(tetrathiafulvalenyl)ethene **7**. **8:** Yellow powder (65%); same NMR data as described above.

Structure Analysis and Refinement. X-ray data were collected at 293 K for **TTF-DMA** and **TTF-VDMA** on a STOE-IPDS diffractometer with monochromatic Mo Kα radiation (λ = 0.71073 Å). General crystallographic data can be found in Table 1. X-ray structure analysis was performed using the WinGX package.[33a] SIR 97[33b] was used for the structure solutions, Shelxl97[34] for the refinements, and Cameron[35] for the production of the crystallographic illustrations. In **TTF-VDMA**, H atoms belonging to the methyl groups of the amino N and those belonging to one TTF moiety were found by difference Fourier maps and refined (coordinates and isotropic temperature factor). Other H atoms as well as all H atoms in **TTF-DMA** were included with their calculated positions and riding on their adjacent atom. Crystallographic data (excluding structure factors) for the structures reported in this paper have been deposited with the Cambridge Crystallographic Data Centre as supplementary publication no. CCDC-622210 (TTF-DMA) and CCDC-622211 (TTF-VDMA). Copies of the data can be obtained free of charge on application to CCDC, 12 Union Road, Cambridge CB2 1EZ, UK (E-mail: deposit@ccdc.cam.ac.uk).

Electrochemical Studies. Cyclic voltammetry data were recorded in acetonitrile, on an Autolab PGSTAT 100 potentiostat, using a Pt disk (1 mm diameter) as the working electrode, a Pt gauze as the auxiliary electrode, and SCE as the reference electrode. nBu_4BF_4 (0.1 M) was used as the supporting electrolyte (purum electrochemical grade Fluka, purified by sublimation). All voltammetric experiments were performed at ambient temperature in a homemade airtight three-electrode cell connected to a vacuum/argon line. The solutions used for the electrochemical studies are 2.5 × 10^{-4} M in TTF species, which allows checking of the UV−visible features in all cases. Prior to measurements, the solutions were deoxygenated via bubbling with argon gas for 15 min and the working electrode was polished with a polishing machine (Presi P230); during experiments, a stream of argon was passed over the solution.

NLO Measurements. The molecular hyperpolarizabilities of **TTF-DMA** and **TTF-VDMA** were estimated by the hyper-Rayleigh scattering (HRS) technique,[36] using a Nd:YAG (Spectra-Physics, GCR 250, 10 ns, 10 Hz) laser. The setup was used as described before,[37] and the solvent was acetonitrile. As a reference compound, *p*-nitroaniline was used with a hyperpolarizability $\beta = 29 \times 10^{-30}$ cm^5 esu^{-1}.[38]

Due to the long duration of the pulses, there is no direct way to distinguish between the possible broad multiphoton fluorescence (MPF) around the second harmonic wavelength (532 nm) and hyper-Rayleigh scattering signal, centered at exactly 532 nm. To determine if a MPF phenomenon is contributing to the HRS signal, the output 2ω light intensities were carefully recorded at 520, 532, and 550 nm, assuming that signals at 520 and 550 nm provide the background MPF contribution to the total (HRS + MPF) signal at 532 nm.

We have obtained the oxidized species by both chemical and electrochemical oxidation of the neutral **TTF-DMA** and **TTF-VDMA** derivatives. The compounds were chemically oxidized by addition of an appropriate amount of iodine to the acetonitrile solutions. In a typical procedure, 1 mL of a 1 × 10^{-4} M solution of neutral TTF derivative in acetonitrile was mixed with 0.2 mL of a 2.7 × 10^{-3} M solution of iodine and diluted to 10 mL. It was carefully checked that no additional HRS signal is due to the presence of iodine in the pure solvent (acetonitrile). The electrochemical oxidation has been performed as described before.[39] Solutions of TTF derivatives (1 × 10^{-5} M) in 0.1 M tetrabutylammonium tetrafluoroborate in acetonitrile were used. A potential of 0.6 V (vs SCE) was applied in all cases, for 10 min. Counter

(32) Bryce, M. R.; Green, A.; Moore, A. J.; Perepichka, D. F.; Batsanov, A. S.; Howard, J. A. K.; Ledoux-Rak, I.; Gonzalez, M.; Martin, N.; Segura, J. L.; Garin, J.; Orduna, J.; Alcala, R.; Villacampa. B. *Eur. J. Org. Chem.* **2001**, 1927.
(33) (a) WINGX, Main Reference, Farrugia, L. J. *J. Appl. Cryst.* **1999**, *32*, 837. (b) Farrugia, L. J. *J. Appl. Crystallogr.* **1997**, *30*, 565.
(34) *Shelxl97*; Anorganische Chemie der Universität: Göttingen, Germany, 1998.
(35) Watkin, D. J.; Prout, C. K.; Pearce, L. J. *Cameron*; Chemical Crystallography Laboratory, University of Oxford: Oxford, England, 1996.
(36) Hendrickx, E.; Clays, K.; Persoons, A. *Acc. Chem. Res.* **1998**, *31*, 675.
(37) (a) Clays, K.; Persoons, A. *Phys. Rev. Lett.* **1991**, *66*, 2980. (b) Clays, K.; Persoons, A. *Rev. Sci. Instrum.* **1992**, *63*, 3285.
(38) Stähelin, M.; Burland, D. M.; Rice, J. E. *Chem. Phys. Lett.* **1992**, *191*, 245.
(39) Asselberghs, I.; Clays, K.; Persoons, A.; McDonagh, A.; Ward, M.; McCleverty, J. *Chem. Phys. Lett.* **2003**, *368*, 408.

Table 2. ZINDO-Calculated Static Hyperpolarizabilities (β_0 in 10^{-30} cm^5 esu^{-1}) with Absorption Maxima (λ_{max} in nm) of $[(TTF-NH_2)_8]^{q+}$ Oligomers at Various Formal ($\rho = q/8$) Oxidation States of TTF Units

system	ρ	$\beta_{(0)}$	λ_{max}
$[(TTF\text{-}NH_2)_8]^{q+}$	0	7.6	240
	$^1/_4$	3891.4	1256
	$^1/_2$	386.5	1302
	$^3/_4$	553.5	2653
	1	232.0	658
$[(TTF\text{-}NH_2)_4]^{4+}$	1	82.0	724
$[(TTF\text{-}NH_2)_2]^{2+}$	1	46.0	861
$TTF\text{-}NH_2$[a]	0	0.6	251

[a] Reference.

electrolyses were performed at a potential of −0.1 V for about 15 mn. The oxidation and reduction processes were monitored by linear spectroscopy to ensure complete oxidation and reduction of the TTF species at these potentials.

Results and Discussion

Hyperpolarizability Charge-Transfer Relationship in Oligomeric TTF Stacks. Changing the charge of a chromophore from $\rho = 0$ to $\rho = 1$ necessarily affects any molecular parameters, such as β, the quadratic molecular hyperpolarizability. Along this line, chemical oxidations have previously been used to achieve convincing NLO switches, for instance, in the case of ruthenium-based metal complexes.[40] On the other hand, NLO properties of chromophores engaged in a fractional ($0 < \rho < 1$) charge-transfer process is a rather unexplored topic, which, to the best of our knowledge, has only been approached by Di Bella et al. in the case of dimeric species, where $\rho = 1/2$.[41]

The calculations performed at zero frequency (β_0 static hyperpolarizabilities) on the noncentrosymmetric stack of 8 $TTF-NH_2$ entities are presented in Table 2, together with the absorption maxima. The NLO response of $[(TTF-NH_2)_8]^0$ and $[(TTF-NH_2)_8]^{8+}$ can readily be related to that of the single $TTF-NH_2$ and $TTF-NH_2^+$ entities. The octameric $[(TTF-NH_2)_8]^0$ system exhibits a β_0 value of 7.6×10^{-30} cm^5 esu^{-1}, in relation to a pseudo-centrosymmetric electronic structure, which approximately corresponds to 8 times the 0.6×10^{-30} cm^5 esu^{-1} β_0 value of the single $TTF-NH_2$ entity, therefore without any significant β enhancement due to TTF···TTF contacts. This absence of π-overlap contribution to β is further supported by the examination of the absorption maxima, which turn out to lie in the same wavelength magnitude (240−251 nm), the main difference being observed in the relative intensities (oscillator strength f) equal to 2.0 and 0.39, for $[(TTF-NH_2)_8]^0$ and $TTF-NH_2$, respectively. In the case of the fully oxidized $[(TTF-NH_2)_8]^{8+}$ ($\rho = 1$) system, the data gathered in Table 2 indicate a β_0 value of 232.0×10^{-30} cm^5 esu^{-1}, 30 times larger than that of the related $[(TTF-NH_2)_8]^0$ system. Two effects can readily account for this enhancement: (*i*) a large red shift and (*ii*) a more pronounced "push−pull" character upon TTF oxidation. Indeed, and within the framework of the crude, but widely used, "two-level" description of the NLO response, a red shift from 240 to 658 nm in the absorption maxima leads to a 20 times β_0 enhancement according to the following equation:[42]

$$\beta_{0(zzz)} = \frac{3e^2\hbar f \Delta\mu_z}{2mE^3}$$

where the static β_0 is assumed to arise from a single transition of energy E, intensity f, and dipole moment change $\Delta\mu$, along the z direction. Additionally, the electron distribution in $TTF-NH_2$ is broken by the oxidation process, leading to a "push−pull" electronic character (larger $\Delta\mu$ value) between the electron-rich $-NH_2$ substituent and the acceptor TTF^+ unit. The β calculation is not available with the commercial ZINDO packaged for "open-shell" structures. However, we have checked the evolution of the β values for "close-shell" $[(TTF-NH_2)_2]^{2+}$, $[(TTF-NH_2)_4]^{4+}$, and $[(TTF-NH_2)_8]^{8+}$ systems (Table 2). A slight lowering of λ_{max} is observed as the size of the stack increases (from 861 to 658 nm). However, β_0 per TTF unit turns out not to be significantly influenced by the size of the oligomeric stack. With this respect, the NLO response of $[(TTF-NH_2)_8]^{8+}$ appears to derive from that of the parent $TTF-NH_2^+$ entity.

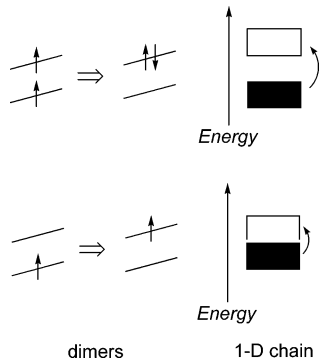

Figure 2. Electron transfer in TTF^+ species, where $\rho = 1$ (top), and in $TTF^{\rho+}$ species, where $\rho = 1/2$ (bottom). The situation depicted on the left is related to discrete dimeric entities, and that on the right is related to one-dimensional stacks.

The situation encountered for TTF bearing fractional charges requires a more careful examination. As ZINDO calculations of β require close-shell electronic structure, the charge of the $[(TTF-NH_2)_8]^{q+}$ oligomers must be equal to 2, 4, and 6 so that the fractional charge ρ is equal to $^1/_4$, $^1/_2$, and $^3/_4$. At first, one might expect that this situation leads to NLO properties lying somewhere between those of the neutral $[(TTF-NH_2)_8]^0$ and oxidized $[(TTF-NH_2)_8]^{8+}$ octamers. In fact, the data gathered in Table 2 indicate that the absorption maxima are deeply switched to longer wavelength values in partially oxidized species, which corresponds to the appearance of new intervalence $TTF^0-TTF^+ \rightarrow TTF^+-TTF^0$ charge-transfer transitions, according to the model depicted in Figure 2. The case of $[(TTF-NH_2)_8]^{2+}$ deserves special interest, with a β value of 3891×10^{-30} cm^5 esu^{-1}. To further analyze the origin of this intriguingly

(40) (a) Coe, B. J. *Acc. Chem. Res.* **2006**, *39*, 383. (b) Coe, B. J.; Houbrechts, S.; Asselberghs, I.; Persoons, A. *Angew. Chem., Int. Ed.* **1999**, *38*, 366.

(41) Di Bella, S.; Fragalà, I.; Marks, T. J.; Ratner, M. A. *J. Am. Chem. Soc.* **1996**, *118*, 12747.

(42) (a) Oudar, J. L. *J. Chem. Phys.* **1977**, *67*, 446. (b) Oudar, J. L.; Chemla, J. *J. Chem. Phys.* **1977**, *66*, 2664.

Table 3. (a) Main Transitions (λ_{max} in nm, Oscillator Strengths *f*, Dipole Moment Change in *D*) over 400 Involved in the NLO Response of $[(TTF{-}NH_2)_8]^{2+}$ with (b) Relative Contribution of the Main Excitations between Orbitals

(a)

transition i	λ_{max}	f	$\Delta\mu$	%[a]	composition[b] of C.I. expansion
$1 \rightarrow 8$	1260	12.9	2.2	42	$0.924\chi_{231\rightarrow232}$
$1 \rightarrow 10$	1178	0.5	37.0	24	$0.773\chi_{224\rightarrow232} - 0.404\chi_{222\rightarrow232} + 0.381\chi_{223\rightarrow232}$
$1 \rightarrow 16$	1060	0.2	17.4	12	$0.648\chi_{221\rightarrow232} + 0.511\chi_{220\rightarrow232} - 0.450\chi_{222\rightarrow232}$
$1 \rightarrow 4$	2383	0.2	17.4	8	$0.830\chi_{229\rightarrow232} + 0.491\chi_{225\rightarrow232}$
other 396				14	

(b)

excitation	contribution	excitation	contribution
1. $\chi_{231\rightarrow232}$	1.000[c]	5. $\chi_{221\rightarrow232}$	0.050
2. $\chi_{224\rightarrow232}$	0.398	6. $\chi_{223\rightarrow232}$	0.035
3. $\chi_{229\rightarrow232}$	0.055	7. $\chi_{220\rightarrow232}$	0.031
4. $\chi_{222\rightarrow232}$	0.053	8. $\chi_{225\rightarrow232}$	0.019

[a] $\% = \dfrac{f_i \times \Delta\mu_i/E_i^3}{\sum_i (f_i \times \Delta\mu_i/E_i^3)}$ [b] Orbital 231 is the HOMO and orbital 232 the LUMO in $[(TTF{-}NH_2)_8]^{2+}$. [c] Normalized to 1 for $\chi_{231\rightarrow232}$

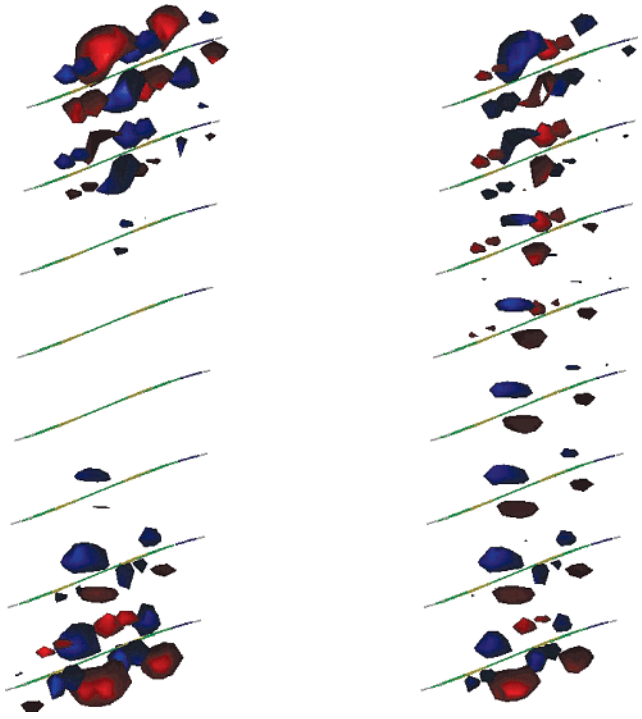

Figure 3. HOMO (left) and LUMO (right) in $[(TTF{-}NH_2)_8]^{2+}$.

large value, and in the framework of the SOS perturbation theory,[28] it must be reminded that β is expressed as the sum of two contributions ($\beta = \beta_{2level} + \beta_{3level}$). In the present case, β_{2level} is the dominant part of β, which leads to the assumption that $\beta \equiv \beta_{2level}$, and allows the NLO response to be related to the contribution of the 400 transitions involved in the calculation. Within this approach, the main transitions contributing to β are gathered in Table 3. The data reveal that an extremely intense ($f = 12.9$) HOMO−LUMO based $1 \rightarrow 8$ transition is responsible for 42% of the NLO response, providing a qualitative understanding of the charge-transfer process. The frontier orbitals are shown in Figure 3 and confirm the electron delocalization over the entire extent of the octamer, by means of π-stacking between the TTF

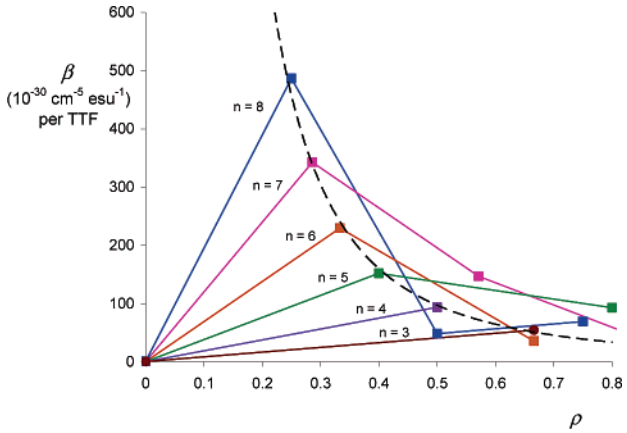

Figure 4. Hyperpolarizabilities per TTF (β/n) for various $[(TTF{-}NH_2)_n]^{q+}$ oligomeric stacks, drawn against the fractional ($\rho = q/n$) oxidation states. The dotted line indicates the evolution of the β values in the case of weak ($q = 2$) oxidation.

Table 4. NLO Response (β in 10^{-30} cm^5 esu^{-1}) for $[(TTF{-}NH_2)_n]^{2+}$ Octamers of Various Sizes (n) with Related Absorption Maxima (λ_{max} in nm)

		NLO response		absorption maxima		
n	ρ	β	β/n	λ_{max}	f	f/n
3	0.666	163	54	1181	1.60	0.533
4	0.500	374	94	1184	3.09	0.772
5	0.400	759	152	1195	4.86	0.972
6	0.333	1377	229	1213	7.04	1.173
7	0.286	2399	343	1235	9.65	1.379
8	0.250	3891	486	1260	12.87	1.609

species. At first glance, the electron density seems to be symmetrically distributed along the stack, but a more careful examination reveals that the dominant electron density is located on different sides of the stack in the two orbitals (top of Figure 3 at the HOMO level and bottom at the LUMO level), providing the "push−pull" charge-transfer effect ($\Delta\mu = 2.2$ D), and hence the large NLO response. Interestingly, other transitions exhibit extremely large $\Delta\mu$ values (Table 3). However, the associated charge-transfer processes do not contribute efficiently to β because of a modest intensity (f).

The extremely large β value obtained for the lowest oxidation state ($\rho = 1/4$) in the present TTF stack encouraged us to study the more general case of $[(TTF{-}NH_2)_n]^{q+}$ ($n = 2{-}8$; $q < n$), which leads to various values of the fractional charge ($\rho = q/n$). The data are shown in Figure 4 as the β values per TTF plotted against ρ. Two intriguing behaviors appear from the figure: (*i*) $[(TTF{-}NH_2)_n]^{2+}$ provides the largest β value for a given oligomer, whatever the size (n) of the stack and (*ii*) reducing the fractional oxidation state provides a dramatic β enhancement (dotted curve in Figure 4). This latter result could motivate the investigation of more extended ($n > 8$) oligomeric stacks. On the other hand, the issue of efficiency/transparency tradeoff becomes naturally addressed in large size $[(TTF{-}NH_2)_n]^{2+}$ oligomeric stacks, together with the challenging issue of their solid-state engineering. While the synthetic feasibility of such species will be evaluated in the last part of the manuscript, the issue of transparency can readily be addressed through an examination of the data gathered in Table 4.

In solid state nonlinear optics, the relevant parameter is not β, but rather β/n, which quantifies the NLO response per volume unit, and hence the potential NLO efficiency of

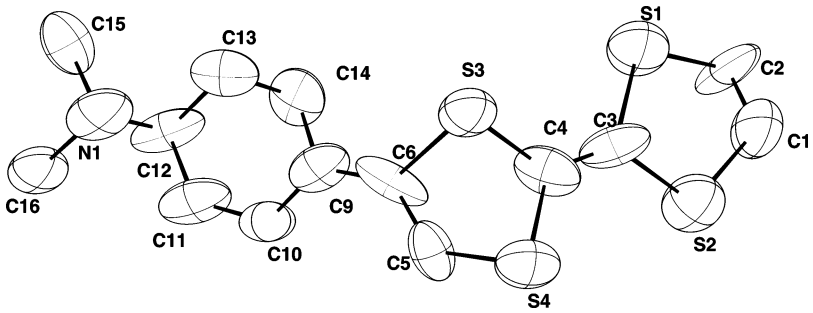

Figure 5. Asymmetric unit cell and atom labeling for TTF-DMA. H atoms are omitted for clarity.

the device. Similarly, the absorbance of the device arises from f/n instead of f. It clearly appears from Table 4 that β/n is strongly enhanced with the size (n) of the stack. Furthermore, λ_{max} is only slightly increased with the size of the $[(TTF-NH_2)_n]^{2+}$ oligomer, which indicates that the β enhancement is not due to a simple red shift induced by long-range electron delocalization, but also by the enhancement of the transition intensity (f/n) at λ_{max}, the device retaining some transparency on a large frequency range, in the near-IR domain. Along this line, designing oligomeric stacks with large n values becomes a challenging target for synthetic chemists. As a first step toward this goal, the search for novel donor-substituted TTF chromophores will be discussed in the next section.

Investigation into the Synthesis of Donor-Substituted TTF Derivatives. TTF and its numerous derivatives have provided many organic materials exhibiting specific conducting,[14] magnetic,[43,44] and optical properties.[18,45,46] In this latter class, TTF-based NLO chromophores are invariably built up from TTF units linked to aromatic acceptors, which allows "push−pull" charge-transfer capabilities and hence sizable NLO responses. By contrast, the present investigation points out the potential interest of donor-substituted TTF species, with the underlying issue of their synthetic feasibility. In this context, we report here on strategies aimed at designing TTF-aniline and TTF-vinylaniline derivatives.

The strategies toward the TTF-dimethylaniline (**TTF-DMA**) **4** are illustrated in Scheme 2 and are based on an organometallic cross-coupling reaction between a tributylstannyl-TTF derivative and a *p*-halogeno-aromatic compound,[22a,4747] whereas the TTF-vinyldimethylaniline (**TTF-VDMA**) **8** (Scheme 3) was obtained from Wittig-type condensations[46−48] between the TTF-carboxaldehyde precursor **5** and an appropriate triphenylphosphonium salt.[31b]

Concerning the **TTF-DMA 4a** (R = R′ = H), a first attempt involving a palladium-catalyzed Stille cross-coupling reaction between the tributylstannyl-TTF **1a**[22a] and the commercially available *p*-bromo-*N*,*N*-dimethylaniline (route a) was tried. However, and as expected with a halogenoaromatic reagent bearing an electron-donating dimethylamino group, this reaction led to a low yield (12%), and moreover turned out not to be fully reproducible so that the route was abandoned.

A Suzuki cross-coupling reaction between the iodotetrathiafulvalene **1′**[23] and the *p*-(dimethylamino)phenylboronic acid was then used (route b), leading to a modest improvement of the yield (22%).

Finally, a multistep procedure (route c) was envisioned, offering much better overall yields (44−50%) from the appropriate tributylstannyl-TTF derivatives **1b** and **1c**,[22b,c] and the *p*-nitrobenzene as a reagent. In this case, the strong electron-withdrawing nitro group increased the reactivity of the Stille reaction, and the donor−acceptor entities **2b** (R = R′ = CH_3) and **2c** (R = CH_3, R′ = H) were isolated in very high yields (98 and 96%, respectively). In the second step of the synthetic process the nitro derivatives **2** were reduced into the corresponding amino compounds **3** in quite good yields (**3b**: 62%; **3c**: 65%). Finally the amino species **3** were successfully converted (74−78%) into the target *N*,*N*-dimethylated molecules **4** by a classical dialkylation reaction using an excess of dimethyliodide in a basic medium.

On the other hand, the more conjugated **TTF-VDMA** derivative **8** was first similarly synthesized (Scheme 3) in a multistep sequence (route a′) involving, in the first step, the Wittig-type condensation described in the literature.[31b,48] As expected, the reaction between the *p*-nitrobenzyltriphenylphosphonium bromide and TTF-carboxaldehyde[24] in the presence of triethylamine led to **6** in a quite high yield (73%). The nitro compound **6** was then easily converted into **7**, which was finally dialkylated to give the target *N*,*N*-dimethylated molecule **8** (65%).

Interestingly, compound **8** was also obtained in one step in 44% yield through a Wittig condensation between the (*p*-dimethylaminobenzyl)triphenylphosphonium bromide[25] and the TTF-carboxaldehyde **5** (route b′).

Structure Description. TTF-DMA crystallizes in the $P2_1$ monoclinic space group. The structure is built up from two nearly planar **TTF-DMA** molecules per cell, which refer to each other through a helicoidal 2_1 axis. The angle between the two **TTF-DMA** mean planes is equal to 80.9°, within the cell. The shortest intermolecular distance is equal to 2.79(4) Å, between C3 and H2. The asymmetric unit cell with atom labeling is shown in Figure 5. The $C_6H_3S_4$ TTF moieties are very slightly bent with largest distances of 0.239 and 0.233 Å observed from a mean plane at H5 (C5) and H2

(43) Ouahab, L. *Chem. Mater.* **1997**, *9*, 1909.
(44) Coronado, E.; Galan-Mascaros, J. R.; Gomez-Garcia, C. J. *Nature* **2000**, *408*, 447.
(45) Ashwell, G. J. *J. Mater. Chem.* **1999**, *9*, 1991.
(46) Andreu, R.; Malfant, I.; Lacroix, P. G.; Cassoux, P. *Eur. J. Org. Chem.* **2000**, 737.
(47) Bouguessa, S.; Hervé, K.; Golhen, S.; Ouahab, L.; Fabre, J. M. *New J. Chem.* **2003**, *27*, 560.
(48) (a) Gonzalez, M.; Martin, N.; Segura, J. L.; Soane, C.; Garin, J.; Orduna, J.; Alcala, R.; Sanchez, C.; Villacampa. B. *Tetrahedron Lett.* **1999**, *40*, 8599. (b) Gonzalez, M.; Martin, N.; Segura, J. L.; Soane, C. *Tetrahedron Lett.* **1998**, *39*, 3051.

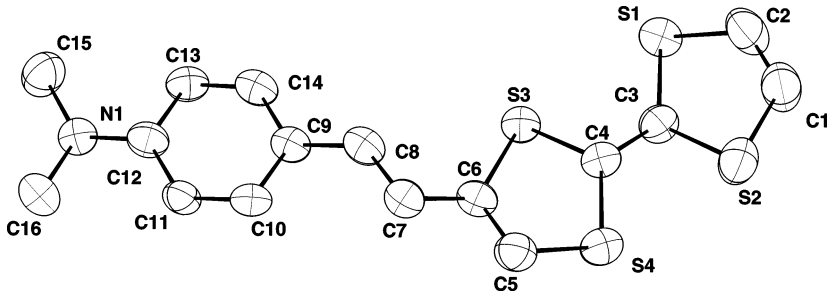

Figure 6. Asymmetric unit cell and atom labeling for TTF-VDMA. H atoms are omitted for clarity.

Table 5. Electrochemical Data (*E* in Volt vs SCE) for TTF-DMA and TTF-VDMA, Compared to Those of the Parent TTF Molecule

	$[TTF\text{-}R] \rightarrow [TTF\text{-}R]^+$		$[TTF\text{-}R]^+ \rightarrow [TTF\text{-}R]^{2+}$		$[TTF\text{-}R]^{2+} \rightarrow [TTF\text{-}R]^{3+}$	
	$E_{1/2}$	ΔE	$E_{1/2}$	ΔE	$E_{1/2}$	ΔE
TTF-DMA	0.33	0.06	0.70	0.06	1.22	0.06
TTF-VDM A	0.36	0.06	0.69	0.06	0.99	0.07
TTF	0.36	0.06	0.75	0.06		

(*C*2), respectively. The angle between the C_6H_4 phenyl plane and the TTF plane is equal to 5.8°. Similarly, **TTF-VDMA** crystallizes in the $P2_1$ space group, with two molecules per cell. The asymmetric unit cell with atom labeling is shown in Figure 6. The shortest intermolecular distance (2.724()Å) is also observed between C3 and H2. In this respect, both crystal structures appear similar. The TTF moieties are slightly more planar than those in **TTF-VDMA**, with a largest distance of 0.128 Å from the mean plane observed at H(5). The angle between TTF and the C_6H_4 plane is equal to 7.3°.

Electrochemical Studies. Cyclic voltammetry measurements were performed to fully characterize the redox properties of **TTF-DMA** and **TTF-VDMA**, in relation to those of the parent **TTF** molecules. The data are presented in Table 5, and a representative voltammogram is shown in Figure 7, in the case of **TTF-DMA**.

Both **TTF-DMA** and **TTF-VDMA** exhibit three fully reversible oxidation processes, the first two being reminiscent of those observed in **TTF**, and an additional one around 1 V, being likely ascribable to the oxidation of the aniline fragment. The full reversibility of the redox processes indicates that the optical (UV−visible) and hence nonlinear optical properties (HRS measurements) of the TTF species should be accessible in both 0 and +1 oxidation states.

Optical Properties. The UV−visible electronic spectra of **TTF-DMA** and **TTF-VDMA**, recorded in acetonitrile, are shown in Figure 8. In both cases, the spectra indicate two dominant bands with absorption maxima at 322 (28200) and 382 (5900) for **TTF-DMA** and at 358 (36800) and 400 nm (18000 mol^{-1} L cm^{-1}) for **TTF-VDMA**. The slight red shift and increased intensity observed at a longer path of conjugation is a general tendency in π-electronic structures. We have observed that the oxidation of the TTF species leads to a significant modification of the color from orange (**TTF-DMA**) and orange-red (**TTF-VDMA**) to green in solution in acetonitrile. This spectroscopic change is observed in both derivatives and is exemplified in Figure 9, in the case of **TTF-DMA**. Previous spectroscopic investigations conducted on TTF^0 and TTF^+ salts have pointed out that the two bands of TTF^0 observed around 300 nm (λ_{max}) and 400 nm (low-

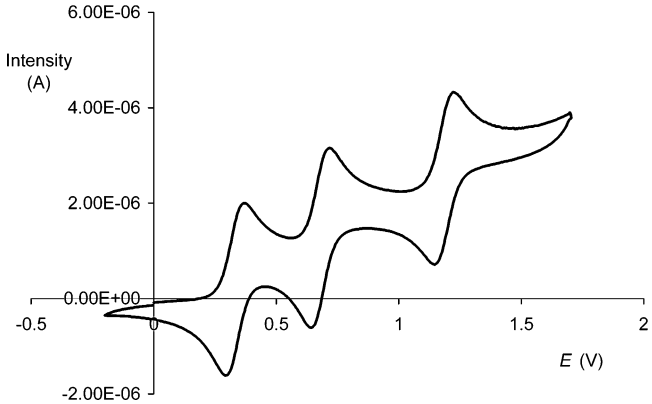

Figure 7. Cyclic voltammogram of TTF-DMA in CH_3CN, at room temperature, with 0.1 M nBu_4BF_4 as supporting electrolyte (Pt electrode, r = 0.5 mm), scan rate = 0.1 V s^{-1}. The E values are vs SCE.

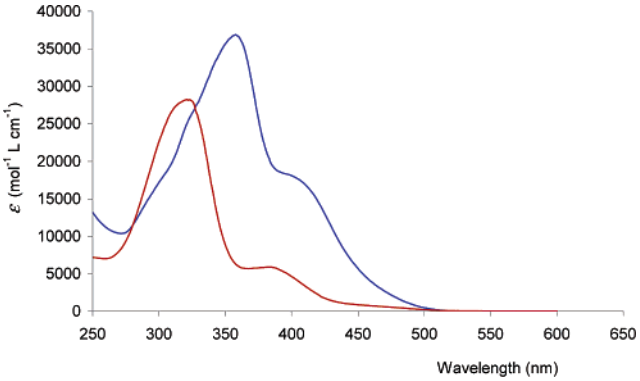

Figure 8. UV−visible electronic spectra of TTF-DMA (red) and TTF-VDMA (blue), recorded in acetonitrile.

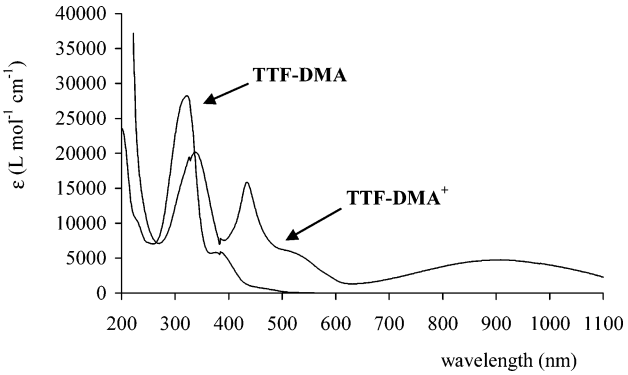

Figure 9. UV−visible electronic spectra of TTF-DMA and $[TTF\text{-}DMA]^+$ in acetonitrile.

Scheme 4

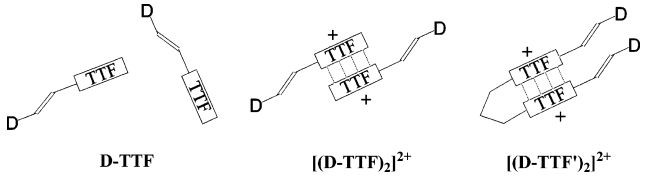

intensity transition) lead to three bands located at 340, 430, and 580 nm, after oxidation.[49,50] Interestingly, these spectroscopic features find their counterpart in Figure 9. Furthermore, the presence of dimeric $[(TTF)_2]^{2+}$ entities in solution has been reported to lead to the appearance of an additional and broad transition lying from 600 to 1000 nm.[49] Although this low-lying band is slightly red-shifted, its presence in our case supports the trend for strong dimeric interactions in both **TTF-DMA**$^+$ and **TTF-VDMA**$^+$ species, as illustrated in Scheme 4 (left and middle). The consequence of these interactions will be investigated in the next section.

Hyper Rayleigh Scattering Measurements. The NLO responses have been evaluated at 1.064 μm by the HRS technique. In both neutral derivatives, the HRS signals were found not to be contaminated by any multiphoton fluorescence (MPF). This leads to dynamic β_{zzz} values of 240 and 236 $\times$ 10^{-30} ($\pm$15%) cm^5 esu^{-1} for **TTF-DMA** and **TTF-VDMA**, respectively. The presence of an electronic resonance (UV$-$vis absorption at 382 and 400 nm, respectively) leads to so-called resonance enhancement factors of 2.37 and 2.68, respectively. The resonance-free, so-called static β_{zzz} values amount to 100 and 87 $\times$ 10^{-30} cm^5 esu^{-1}, respectively ($\pm$5%). Within statistical error, these values are identical. The origin of these rather large values is somewhat unclear and might tentatively be partially related to the large size of the molecules (17 Å in **TTF-VDMA**). Please note that the molecule is noncentrosymmetrical: even if both the **TTF** and **DMA** moieties are electron donors, the cyclic voltammetry studies evince the **TTF** and **DMA** do not exhibit the same electron-donating strength (first oxidation of TTF around 0.36 V and oxidation of DMA moiety around 1 V). This difference in electron-donating strength results in an effective noncentrosymmetry for TTF-DMA and TTF-VDMA, as evidenced by the sizable second-order hyperpolarizabilty. No further investigations were conducted to analyze the NLO response of these neutral molecules.

The first measurements performed on the oxidized **TTF-DMA**$^+$ and **TTF-VDMA**$^+$ species indicate very large HRS signals (suggesting dynamic β_{zzz} values of 2100 and 4100 $\times$ 10^{-30} ($\pm$15%) cm^5 esu^{-1} for TTF-DMA$^+$ and TTF-VDMA$^+$, respectively. However, a careful examination reveals that no significant intensity differences are evidenced in signals recorded at 520, 532, and 550 nm (e.g., 200, 175, and 185 ($\pm$15%) relative intensities for TTF-VDMA, at these wavelengths, respectively). Please note that a pure second-order NLO signal should give rise to a signal at the second-harmonic wavelengths (532 nm) only, while multiphoton fluorescence is expected to give a broad spectral response. This leads to the surprising conclusion that the oxidized species exhibit vanishing second-order NLO properties (see Experimental Section). However, this behavior is consistent with the presence of strongly interacting dimers in pseudo-centrosymmetric conformation, according to the situation depicted in Scheme 4 (middle).

By contrast, the observation of a large signal at 520 and 550 nm is undoubtedly ascribable to an intense multiphoton fluorescence in the donor-substituted TTF$^+$ species. This could be rationalized, with the assumption of centrosymmetrically dimerized "$(TTF)_2^{2+}$" species, taking into account previous reports of such phenomena in "push$-$pull-push" entities, with strong electron donors present at the extremity.[51,52] This unexpected property in TTF derivatives would likely deserve more special attention in future studies.

Engineering of Specific TTF-Based Oligomeric Stacks. The present computational approach gives rise to the potential NLO capabilities of $[(TTF-D)_n]^{2+}$ stacks. Noncentrosymmetric one-dimensional packing of partially oxidized TTF derivatives (e.g., Figure 1) is somewhat difficult to achieve. Nevertheless, recent reports have shown that although not perfectly aligned for NLO purpose, noncentrosymmetric stacks are observed in some cases with noncentrosymmetrically substituted species.[53] Partial oxidations frequently arise from one-dimensional stacks of strongly S$\cdots$S overlapping TTF species, in the solid state. In the present context, the suitable synthetic target should not be regular stacks, but distorted (e.g., tetrameric or octameric), and furthermore noncentrosymmetric stacks sharing a +2 charge per oligomer. It is well-known that regular stacks of partially oxidized π-overlapping donor species (e.g., TTF) are subjected to structural instabilities, leading to the so-called Peierls distortion,[54] solid state analogue of the molecular Jahn$-$Teller Effect.[55] The driving force accounting for this behavior is the energy lowering resulting from the appearance of a gap of forbidden energy (E) in the band structure, as illustrated in Figure 10. Interestingly, the stabilization of TTF stacks is more pronounced in the case of TTF oligomers carrying a global +2 charge (e.g., $(TTF^+)_2$, $(TTF^{1/2+})_4$, ...) as illustrated in the figure. This is of particular interest, taking into account the fact that this situation leads to the more promising NLO chromophores, according to Figure 4.

Engineering of molecular entities in a specific solid-state environment is a highly laborious target, with the outcome of many uncertain synthetic efforts. To favor intermolecular interactions at the scale of a few TTF units, a strategy could

(49) Torrance, J. B.; Scott, B. A.; Welber, B.; Kaufman, F. B.; Seiden, P. E. *Phys. Rev. B* **1979**, *19*, 730.
(50) Hünig, S.; Kiesslich, G.; Quast, H.; Scheutzow, D. *Liebigs Ann. Chem.* **1973**, 310.
(51) Albota, M.; Beljonne, D.; Brédas, J. L.; Ehrlich, J. E.; Fu, J. Y.; Heikal, A. A.; Hess, S. E.; Kogej, T.; Levin, D. M.; Marder, S. R.; McCord-Maughon, D.; Perry, J. W.; Röckel, H.; Rumi, M.; Subramaniam, G.; Webb, W. W.; Wu, X. L.; Xu, C. *Science* **1998**, *281*, 1653.
(52) (a) Ventelon, L.; Charier, S.; Moreaux, L.; Mertz, J.; Blanchard-Desce, M. *Angew. Chem., Int. Ed.* **2001**, *40*, 2098. (b) Werts, M. H. V.; Gmouh, S.; Mongin, O.; Pons, T.; Blanchard-Desce, M. *J. Am. Chem. Soc.* **2004**, *126*, 16294.
(53) (a) Fujiwara, H.; Hayashi, T.; Sugimoto, T.; Nakazumi, H. Noguchi, S.; Li, L.; Yokogawa, K.; Yasuzuka, S.; Murata, K.; Mori, T. *Inorg. Chem.* **2005**, *45*, 5712. (b) Matsumoto, T.; Komionami, T.; Ueda, K.; Sugimoto, T.; Tada, T.; Noguchi, S.; Yoshino, H.; Murata, K.; Shiro, M.; Negishi, E.; Toyota, N.; Endon, S. Takahashi, K. *Inorg. Chem.* **2002**, *41*, 4763.
(54) Peierls, R. E. *Quantum Theory of Solids*; Oxford University Press: Oxford, 1955; p 108.
(55) Jahn, H. A.; Teller, E. *Proc. R. Soc. London A* **1937**, *161*, 220.

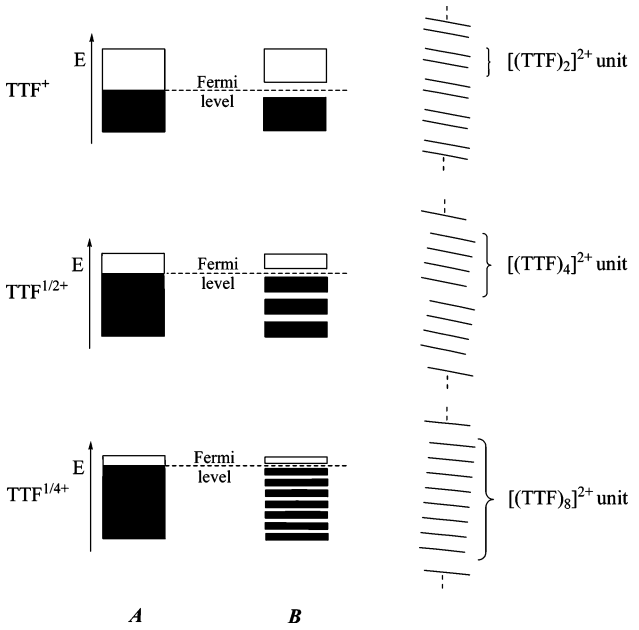

Figure 10. Band structures in chains of TTF^{+} (top), $TTF^{1/2+}$ (middle), and $TTF^{1/4+}$ (bottom), in the case of regular (*A*) or distorted (*B*) one-dimensional structures. The stacks depicted on the right are related to bands *B* and lead to the best stabilization of the (*E*) electronic energy.

be developed to design covalently linked TTF species. For instance, substituted-TTF oligomers containing up to four monomeric species,[16,56] linked by short aliphatic organic chains, have previously been reported. Such species would ensure the noncentrosymmetric conformation required for NLO purpose, as exemplified in the case of a $[(D\text{-}TTF')_2]^{2+}$ species, in Scheme 4 (right). Interestingly, electrochemical data recorded on these covalently banded units reveal very strong TTF···TTF interactions upon oxidation in solution.

Conclusion

TTF-dimethylaniline and TTF-vinyldimethylaniline have been synthesized in reasonably good yield (about 50%), and fully characterized. These molecules possess the unusual "$donor_1$−bridge−$donor_2$" π-electronic structure. They were studied to illustrate the synthetic feasibility of donor-substituted TTF, after the computational prediction that partially oxidized $TTF-NH_2$ oligomeric stacks would provide the opportunity to obtain giant NLO response.

The potential switch of the static hyperpolarizability (β_0) from 7.6 to 3891.4×10^{-30} cm^5 esu^{-1} in a benchmark species by $[(TTF-NH_2)_8] \rightarrow [(TTF-NH_2)_8]^{2+}$ two electron oxidation raises the intriguing possibility of β optimization by means of partial charge-transfer processes, a strategy which to date has received very little attention. Our investigation has pointed out several important issues, which should be addressed before considering these systems as operating NLO chromophores, the main one being related to the engineering of the interacting TTF species in a suitable environment. In particular, isolated donor-TTF chromophores exhibit a strong tendency for dimerization as pseudo-centrosymmetric [donor−$(TTF)_2$−donor]$^{2+}$ cations after oxidation, a possibility which has to be avoided for NLO purposes, although it could provide a new class of efficient two-photon emitters. To ensure the desirable noncentrosymmetry of the oligomeric stacks, a strategy based on covalently linked donor−TTF precursor is currently under investigation.

CM0623110

(56) Carcel, C.; Fabre, J. M. *Synth. Met.* **2001**, *120*, 747.